JOURNAL OF COMPUTATIONAL PHYSICS 18, 284–299 (1975)

A New Finite Element Approach to the Normal Mode Analysis in Magnetohydrodynamics

K. APPERT, D. BERGER, R. GRUBER, AND J. RAPPAZ

École Polytechnique Fédérale, Centre de Recherches en Physique des Plasmas, 21, av. des Bains, CH–1007 Lausanne, Switzerland

Received August 13, 1974; revised March 11, 1975

The eigenvalue problem arising in the one-dimensional normal mode analysis of fixed boundary magnetohydrodynamic stability is solved by a finite element method. Piecewise constant, discontinuous basis functions are used for two components of the displacement vector because this permits an accurate representation of the nearly divergence-free property of the modes being treated. In spite of the simple basis functions, the accuracy is greatly improved compared to that obtained with piecewise linear, continuous basis functions. Important features of the spectrum, such as infinitely degenerated eigenvalues, accumulation points, and continua are well represented by the method. The method used is equally well applicable to the free boundary stability problem.

I. INTRODUCTION

The finite element method has recently been proposed by Ohta *et al.* [1] as a tool for the analysis of magnetohydrodynamic stability of a current-carrying plasma. Since then, several authors [2, 3, 4] have applied the method to infinitely long, axisymmetric plasmas. The problem to be solved in this case is a one-dimensional, linear, self-adjoint eigenvalue problem of second order for a displacement vector ξ with three components ξ_r, ξ_θ, ξ_z. It has been shown analytically that the full spectrum of eigenvalues may contain continuous parts [5–13], accumulation points [12, 13] or distinct infinitely degenerate eigenvalues [12, 13]. So it is not astonishing that the standard choices of basis functions [1–4], e.g., piecewise linear or cubic functions for all components of ξ, may not be the best. In fact, the choice of linear basis functions destroys the degeneracy of the Alfven-oscillations in a homogeneous currentless plasma cylinder [4]. The corresponding numerical results have a Bessel-function-like shape, which is attributable to the discretization and not to physics. The same discretization errors make it impossible to find the correct shape of the unstable modes in a fixed boundary Tokomak, although the eigenvalue of the most unstable mode can be obtained [2].

In a very recent report [14] a finite element method has been applied to a two-dimensional problem, in which the eigenvalues and eigenfunctions of the most unstable kink modes have been successfully determined. It has not been shown that this method is capable of determining the growth rates of weakly unstable modes. The difficulty lies in the fact that the expression of the potential energy contains positive definitive terms which in fact are always very small. If these terms are not correctly represented by the finite elements, they overcompensate the destabilizing term, thereby introducing errors.

We shall show that these defects of the method disappear in one-dimensional problems if a more appropriate choice of the basis functions is made. Since the variational form of the eigenvalue problem contains only first derivatives of ξ_r [2], discontinuous basis functions are admissible for the components ξ_θ and ξ_z. Our choice then is determined by a physical argument. Because unstable modes are nearly incompressible, the displacement $\boldsymbol{\xi}$ should be approximated within a function class where incompressibility can well be represented. So we are led to a special combination of piecewise linear and piecewise constant basis functions. It is noteworthy that despite the use of simpler functions, the convergence properties are improved.

II. The Physical Problem

Consider a small, time and space dependent displacement $\boldsymbol{\xi}$ of a perfectly conducting fluid in magnetohydrostatic equilibrium. The equation of motion for $\boldsymbol{\xi}$ is given by [15]

$$\rho \frac{\partial^2 \boldsymbol{\xi}}{\partial t^2} = \mathbf{F}(\boldsymbol{\xi}) \equiv \nabla(\boldsymbol{\xi} \cdot \nabla p + \gamma p \nabla \cdot \boldsymbol{\xi}) + (\nabla \times \mathbf{Q}) \times \mathbf{B} + (\nabla \times \mathbf{B}) \times \mathbf{Q}, \quad (1)$$

where $\mathbf{Q} = \nabla \times (\boldsymbol{\xi} \times \mathbf{B})$. Here $\rho(\mathbf{r})$, $p(\mathbf{r})$, and $\mathbf{B}(\mathbf{r})$ denote equilibrium quantities, the mass density, the pressure, and the magnetic field, respectively. γ is the adiabaticity index. The equilibrium quantities satisfy the relation

$$(\nabla \times \mathbf{B}) \times \mathbf{B} = \nabla p. \quad (2)$$

A current way to attack the stability problem in an axisymmetric infinitely long plasma is to look for normal mode solutions to Eq. (1) of the form

$$\boldsymbol{\xi}(\mathbf{r}) = \boldsymbol{\xi}(r)\, e^{i(\omega t + m\theta + kz)}, \quad (3)$$

constrained by the boundary conditions

$$\boldsymbol{\xi}(0) \quad \text{finite}, \qquad \xi_r(R) = 0, \quad (4)$$

where R is the radius of a bounding impenetrable wall. ξ_r, ξ_θ, ξ_z are the components of $\boldsymbol{\xi}$ in cylindrical coordinates. Under these assumptions the equation of motion, Eq. (1), may be brought to the variational form of Newcomb [16], i.e., the stationary point formulation [17] of the eigenvalue problem

$$\omega^2\delta\int\rho\,|\,\boldsymbol{\xi}\,|^2\,r\,dr=\delta\int\left\{\Lambda\left(\xi_r,\frac{d\xi_r}{dr}\right)+\gamma p\left|\,\eta+\frac{1}{r}\frac{d}{dr}(r\xi_r)\right|^2\right.$$
$$\left.+\frac{k^2r^2+m^2}{r^2}\left|\,\zeta-\zeta_0\left(\xi_r,\frac{d\xi_r}{dr}\right)\right|^2\right\}r\,dr. \tag{5}$$

Here,

$$\Lambda\left(\xi_r,\frac{d\xi_r}{dr}\right)=\frac{1}{k^2r^2+m^2}\left|(krB_z+mB_\theta)\frac{d\xi_r}{dr}+(krB_z-mB_\theta)\frac{\xi_r}{r}\right|^2$$
$$+\left[(krB_z+mB_\theta)^2-2B_\theta\frac{d}{dr}(rB_\theta)\right]\frac{\xi_r^2}{r^2}, \tag{6}$$

and

$$\zeta_0\left(\xi_r,\frac{d\xi_r}{dr}\right)=\frac{r}{k^2r^2+m^2}\left[(krB_\theta-mB_z)\frac{d\xi_r}{dr}-(krB_\theta+mB_z)\frac{\xi_r}{r}\right], \tag{7}$$

$$\eta=i(m/r)\,\xi_\theta+ik\xi_z\,,$$
$$\zeta=i\xi_\theta B_z-i\xi_z B_\theta\,. \tag{8}$$

δ denotes the variation of a functional.

In Eq. (5), ξ_r, $i\xi_\theta$, $i\xi_z$ can be taken real without loss of generality [16]. Note that the left- and right-hand sides of Eq. (5) are proportional to the kinetic and the potential energy of the plasma, respectively. From Eq. (5) it is self-evident that the operator $\mathbf{F}(\boldsymbol{\xi})$ in Eq. (1) is self-adjoint at least in the one-dimensional case, and is shown for the general case by Greene and Johnson [18]. Hence the eigenfrequencies ω^2 are real. The plasma is unstable when negative eigenvalues ω^2 exist. Note further that Eq. (5) contains only derivatives on ξ_r.

The energy principle, Eq. (5), was the starting point of many analytical papers on MHD-stability in the last 15 years. In most cases the problem was significantly simplified by determining only the minimum of the potential energy rather than the full solution of Eq. (5). This method (so called δW-method) will give the correct answer for marginal stability ($\omega = 0$), but cannot give correct growth rates as can be seen by the following considerations.

In the δW-method the second and third terms in the potential energy integral in Eq. (5) can be minimized to zero because the first term does not depend on ξ_θ and ξ_z. Hence minimum potential energy implies incompressibility (second term:

div $\xi = 0$) of the unstable modes. Since the adiabaticity index influences the motion, Eq. (1), only in the combination γ div ξ, growth rates calculated with the δW-method do not depend on γ. On the other hand it is known [2, 19] that growth rates may strongly depend on γ. Therefore the δW-method is not appropriate when exact knowledge of the growth rates is required. Bernstein *et al.* [20] were already aware of this fact when originally formulating their energy principle in 1958.

However, the δW-method gives us a hint on how to choose our basis functions when attacking the full stationary point problem, Eq. (5), with the method of finite elements. The form of Eq. (5) implies that div $\xi \approx 0$ and $\zeta - \zeta_0 \approx 0$ for weakly unstable displacements, since these two quantities are exactly zero in the marginal case ($\omega = 0$). Therefore, it should be possible to represent div $\xi = 0$ and $\zeta - \zeta_0$ within the function class chosen. However, by comparison of numerical and analytic results, we found it sufficient that only div $\xi = 0$ be correctly represented. To see why, we reexamine the spectrum of a plasma cylinder of constant density in a homogeneous longitudinal magnetic field B_z [4]. The equation of motion specialized to this case reads:

$$\begin{aligned} -\omega^2 \rho \xi_z &= ik\gamma p \nabla \cdot \xi, \\ -\omega^2 \rho \xi_\perp &= (B_z^2 + \gamma p)\, \nabla_\perp (\nabla \cdot \xi) - ikB_z^2 (\nabla_\perp \xi_z - ik\xi_\perp) \end{aligned} \tag{10}$$

Here $\perp$ denotes vectors perpendicular to the magnetic field. ρ, p, B_z are constant. Particular solutions of Eq. (10), the so-called Alfven-oscillations, can be found by setting

$$\xi_z = 0, \tag{11}$$

so that

$$\nabla \cdot \xi = 0, \qquad (k^2 B_z^2 - \omega^2 \rho)\, \xi_\perp = 0. \tag{12}$$

The eigenvalue

$$\omega^2 = k^2 B_z^2 / \rho \tag{13}$$

is infinitely degenerate, since every ξ_r satisfying the boundary condition, Eq. (4), determines with Eqs. (11) and (12) a nontrivial ξ_θ.

Imagine now a plasma with an additional small B_θ (e.g., Tokomak). It can be shown [2, 21, 22] that, for special values of B_θ, the Alfven-oscillations go unstable. For a good discrete approximation of these instabilities we require the degenerate eigenvalue of the solution without B_θ to be exactly represented by the finite element method. With the method described in [4] we found one-third of the eigensolutions to be badly represented Alfven-modes. Hence the discrete description of Eq. (10) should be chosen in such a way that one-third of the eigenmodes may be purely torsional and incompressible as required by Eqs. (11) and (12).

III. Discretization

Let us carry out the variation in Eq. (5):

$$a(\delta\xi, \xi) - \omega^2 b(\delta\xi, \xi) = 0. \tag{14}$$

Then the problem to be solved may be formulated as follows. Find a scalar ω^2 and a "sufficiently regular" vector ξ satisfying the boundary conditions, Eq. (4), for which Eq. (14) holds whatever "sufficiently regular" $\delta\xi$ satisfying Eq. (4) is taken.

In order to get rid of the apparent singularities induced in Eq. (5) by the cylindrical geometry we define a new displacement vector [23] $\hat{\xi}$ by

$$\hat{\xi} = \begin{pmatrix} \hat{\xi}_1 \\ \hat{\xi}_2 \\ \hat{\xi}_3 \end{pmatrix} = \mathbf{U} \cdot \xi = \begin{pmatrix} \xi_r \\ (\xi_r + \text{im } \xi_\theta)/r \\ i\xi_z \end{pmatrix}. \tag{15}$$

All components of $\hat{\xi}$ are real, because ξ_r, $i\xi_\theta$, $i\xi_z$ may be real. With Eq. (15) we exclude the case $m = 0$ from our further considerations. This case could be treated with the transformation used in [4]. Let us further define

$$\begin{aligned} \hat{a}(\delta\hat{\xi}, \hat{\xi}) &= a(\mathbf{U}^{-1}\,\delta\hat{\xi}, \mathbf{U}^{-1}\hat{\xi}), \\ \hat{b}(\delta\hat{\xi}, \hat{\xi}) &= b(\mathbf{U}^{-1}\,\delta\hat{\xi}, \mathbf{U}^{-1}\hat{\xi}). \end{aligned} \tag{16}$$

Then the problem to be solved is given in Eq. (14), if everywhere the hat is inserted:

$$\hat{a}(\delta\hat{\xi}, \hat{\xi}) - \omega^2 \hat{b}(\delta\hat{\xi}, \hat{\xi}) = 0. \tag{17}$$

The essential structure of the bilinear forms a and $\hat{a}$ is the same: they only contain first derivatives d/dr on ξ_r and $\hat{\xi}_1$, respectively. Hence "sufficiently regular" means that $\hat{\xi}$ belongs to $H = H^1(0, R) \times L_2(0, R) \times L_2(0, R)$, i.e., $\hat{\xi}_1$ belongs to the Sobolev space $H^1(0, R)$ and that $\hat{\xi}_2$ and $\hat{\xi}_3$ are square integrable.

For the numerical treatment of Eq. (17) we need a finite-dimensional (dimension N) subspace V of "sufficiently regular" functions $\hat{\xi}$ with the property explained in the preceding section: V should contain $N/3$ linearly independent functions $\hat{\xi}$ satisfying the two relations

$$\nabla \cdot \xi = \nabla \cdot \mathbf{U}^{-1} \cdot \hat{\xi} = \frac{d\hat{\xi}_1}{dr} + \hat{\xi}_2 + \hat{\xi}_3 = 0, \qquad \hat{\xi}_3 = 0 \tag{18}$$

in every point of the interval $0 \leqslant r \leqslant R$. More accurately, V can be defined in the following way.

Let V_1 be a finite-dimensional subspace of $H^1(0, R)$ of type "finite element" constrained by the boundary conditions, Eq. (4). Let V_2 and V_3 be two finite-dimensional subspaces of $L_2(0, R)$ and having the properties: For all $\xi_1 \in V_1$ there

exists $\xi_2 \in V_2$ and $\xi_3 \in V_3$ such that Eq. (18) holds. V is then defined by

$$V = V_1 \times V_2 \times V_3 . \tag{19}$$

Let us first examine the subspace of "sufficiently regular" functions used in [1–4]. Assume the interval $0 \leqslant r \leqslant R$ to be devided in n subintervals. A piecewise linear (i.e., linear in every subinterval), continuous function is determined by $3n + 1$ nodal values: $n + 1$ nodal values for each component of $\hat{\xi}$ minus the two determined by the boundary condition, Eq. (4). Hence the dimension of the space is $N = 3n + 1$. The number of constraints given by Eq. (18) is also $3n + 1$, since the $n + 1$ nodal values of $\hat{\xi}_3$ and the n pieces of the piecewise linear function $(d\hat{\xi}_1/dr) + \hat{\xi}_2$ have to be identically zero. Consequently no piecewise linear, continuous function $\hat{\xi}$ satisfying Eq. (18) exists. Almost the same is true for piecewise cubic, continuous functions with continuous first derivatives. In this case, the dimension is $N = 6n + 4$ and the number of constraints is $6n + 2$. At most two linearly independent functions may satisfy Eq. (18).

From all possible subspaces V, which contain $N/3$ linearly independent functions satisfying Eq. (18) we choose the simplest one: continuous piecewise linear $\hat{\xi}_1$ and piecewise constant $\hat{\xi}_2$ and $\hat{\xi}_3$. In this space of dimension $3n - 1$ Eq. (18) yields $2n$ constraints. Hence $n - 1$ well-represented Alfven-modes may exist. The basis of V is given by

$$\begin{pmatrix} e_i \\ 0 \\ 0 \end{pmatrix}, \quad i = 0, 1, \ldots, n; \qquad \begin{pmatrix} 0 \\ c_{i+(1/2)} \\ 0 \end{pmatrix}, \begin{pmatrix} 0 \\ 0 \\ c_{i+(1/2)} \end{pmatrix}, \quad i = 0, 1, \ldots, n-1; \tag{20}$$

where e_i are triangular functions as defined in [4] and

$$c_{i+(1/2)}(r) = \begin{cases} 1 & \text{for } r_i < r < r_{i+1}, \\ 0 & \text{elsewhere,} \end{cases} \qquad 0 \leqslant i < n - 1. \tag{21}$$

Here a mesh $0 = r_0 < r_1 < \cdots < r_n = R$ is assumed. The approximation of a displacement $\hat{\xi}$ in the space V reads

$$\hat{\xi} = \sum_{i=0}^{n} x_1 \begin{pmatrix} e_i \\ 0 \\ 0 \end{pmatrix} + \sum_{i=0}^{n-1} \left[x_2^{i+(1/2)} \begin{pmatrix} 0 \\ c_{i+(1/2)} \\ 0 \end{pmatrix} + x_3^{i+(1/2)} \begin{pmatrix} 0 \\ 0 \\ c_{i+(1/2)} \end{pmatrix} \right], \tag{22}$$

where the nodal parameters x_1^i, $x_2^{i+(1/2)}$, $x_3^{i+(1/2)}$ are the values of $\hat{\xi}_1$ at $r = r_i$ and of $\hat{\xi}_2$ and $\hat{\xi}_3$ at $r = r_{i+(1/2)} \equiv (r_i + r_{i+1})/2$. The insertion of Eq. (22) for $\hat{\xi}$ and Eq. (20) for $\delta\hat{\xi}$ in Eq. (17) yields together with Eq. (4) an algebraic eigenvalue problem of dimension $3n - 1$. The integrals necessary to be carried out in Eq. (5) may be performed by using a Simpson-routine.

IV. Applications

The Homogeneous Currentless Plasma Cylinder

First we apply our method to the simple situation described by Eq. (10). With a mesh of n intervals, we find the eigenvalue of the Alfven-branch, Eq. (13), to be $(n-1)$-fold degenerate in contrast to [4]. Because of the degeneracy, no spurious physical structure of the associated eigenvectors as in [4] was observed. These two results were our principal goal when introducing the space V according to Eqs. (19) and (20).

There was a second class of badly described eigensolutions in our previous work, the slow waves, whose eigenvalues are analytically given by

$$\omega_\alpha^2 = \frac{B_z^2}{2\rho R^2}(R^2k^2 + \gamma_{m,\alpha}^2)(1+s^2)\left[1 - \left(1 - \frac{4s^2}{(1+s^2)^2}\frac{R^2k^2}{R^2k^2+\gamma_{m,\alpha}^2}\right)^{1/2}\right], \quad (23)$$

where $s^2 = \gamma p/B_z^2$ and $\gamma_{m,\alpha}$ is the αth zero of $dJ_m(x)/dx$. With increasing α, i.e., increasing $\gamma_{m,\alpha}$, ω_α^2 decreases and tends toward the accumulation point $\omega_\infty^2 =$

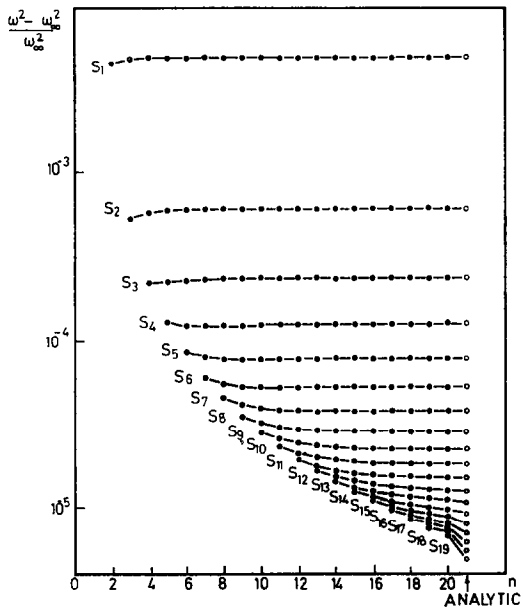

FIG. 1. Numerically calculated spectrum of the slow wave branch in the homogeneous currentless plasma cylinder as a function of the number of intervals. At the right-hand side the first 19 eigenvalues of the exact analytic spectrum are plotted. The wavenumbers are $m = 1$, $k = -0.5$.

$\gamma pk^2/\rho(1 + s^2)$. The frequency band occupied by this class of solutions may be very narrow relative to the value of the accumulation point, which is, in addition, the lowest frequency of the whole spectrum. Figure 1 shows the numerical solution to Eq. (23) as a function of the number n of intervals. The parameters used are $m = 1$, $k = 0.5$, and $s^2 = 1/12$ (plasma with $\beta = 0.1$ and $\gamma = 5/3$).

The modes corresponding to the spectrum of Fig. 1 are well described; once more in contrast to [4]. As an example, we compare in Fig. 2 the numerical solutions for

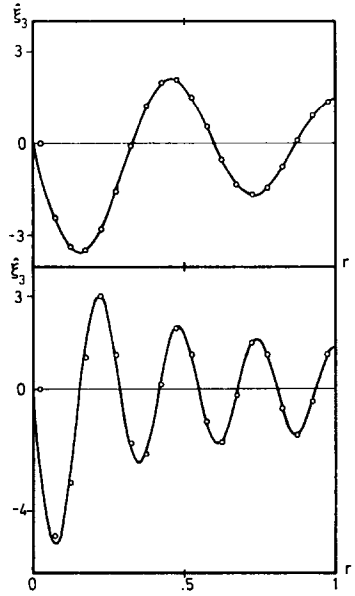

FIG. 2. Analytic (solid line) and numerical (points) solutions to the component $\hat{\xi}_3$ of the slow wave branch. The corresponding eigenvalues are $\omega_4^2 - \omega_\infty^2 = 2.5 \cdot 10^{-6}$ and $\omega_8^2 - \omega_\infty^2 = 5.8 \cdot 10^{-7}$, respectively. The boundary conditions have been used for the innermost point.

the modes corresponding to ω_4^2 and ω_8^2 with the analytic solutions $J_1(\gamma_{1,4}r/R)$ and $J_1(\gamma_{1,8}r/R)$, respectively. In [4] the mode associated with ω_2^2 was badly described, whereas the higher modes could not even be identified. Note that these results can only be obtained in the space V as specified by Eq. (20), whereas the Alfven-class would be degenerate even with linear, continuous ξ_z, since $\xi_z(r) = 0$ for this class.

The Inhomogeneous Currentless Plasma Cylinder (Continuous Spectra)

For several years the continuous spectra of ideal MHD and their associated singular eigenmodes have been discussed in the literature [5–13]. As a test, here

we apply our numerical method to a simple plasma model, which exhibits the two continua possible in a general screw pinch. The model is characterized by

$$B_z = \text{const}, \; B_\theta = 0, \; p = \text{const}, \text{ and } \rho = \rho_0[1 - \epsilon(r^2/R^2)], \qquad \text{where} \quad 0 \leqslant \epsilon \leqslant 1. \tag{24}$$

Equation (10) still holds for this plasma. Let us eliminate ξ_θ and ξ_z from Eq. (10). We then find [19] that

$$\frac{d}{dr}\left[\frac{b_A(r)\, b_S(r)}{N(r)} \frac{1}{r} \frac{d}{dr}(r\xi_r)\right] + b_A(r)\, \xi_r = 0, \tag{25}$$

where

$$\begin{aligned} b_A(r) &= \rho(r)\, \omega^2 - k^2 B_z^2, \\ b_S(r) &= \rho(r)\, \omega^2(\gamma p + B_z^2) - k^2 B_z^2 \gamma p, \\ N(r) &= \rho^2(r)\, \omega^4 - [k^2 + (m^2/r^2)]\, b_S(r). \end{aligned} \tag{26}$$

Equation (25) has solutions with logarithmic singularities at points r_A and r_S, if, somewhere in the interval $0 < r < R$, $b_A(r_A) = 0$ or $b_S(r_S) = 0$. The equation is of Fuchs' type in the neighborhood of such a point. On the other hand, it can be shown [13] that $N(r) = 0$ does not give rise to singular solutions. Note that $b_A(r) = 0$ yields the dispersion relation for the Alfven-class in the limiting case of constant density ($\epsilon = 0$). Similarly, $b_S(r) = 0$ and $\epsilon = 0$ yield the accumulation point ω_∞^2 of the slow waves. Further, by expressing ξ_θ and ξ_z in Eq. (10) in terms of ξ_r, it can be shown, that ξ_θ exhibits a singularity $1/(r - r_A)$ at the points $b_A(r_A) = 0$ and ξ_z in turn a singularity $1/(r - r_S)$ at the points $b_S(r_S) = 0$.

At first glance, one might be puzzled by the existence of singular normal modes. But remember that we are calculating Fourier transforms, Eq. (3), of physical quantities and that a Fourier transform of a well-behaved function may be a distribution, e.g., $\delta(x - \omega)$ is the transform of $\exp(ixt)$. In fact, these singular normal modes with divergent $\int |\xi|^2 r dr$ are not meaningless, if they are associated with a continuous spectrum, which allows well-behaved square-integrable wave-packets to form. Such continua *do* exist, since *every* point, where $b_A(r) = 0$ or $b_S(r) = 0$, gives rise to a singular solution, which satisfies the boundary condition [8, 24]. The two continua are given by

$$\min_{0<r<R} \frac{k^2 B_z^2}{\rho(r)} \leqslant \omega^2 \leqslant \max_{0<r<R} \frac{k^2 B_z^2}{\rho(r)} \qquad \text{(Alfven)} \tag{27}$$

and

$$\min_{0<r<R} \frac{k^2 \gamma p}{\rho(r)(1 + s^2)} \leqslant \omega^2 \leqslant \max_{0<r<R} \frac{k^2 \gamma p}{\rho(r)(1 + s^2)} \qquad \text{(slow wave).} \tag{28}$$

So, the inhomogeneous density distribution spreads the degenerate eigenvalues of the Alfven-waves and the accumulation point of the slow waves to form continua.

Having been successful in the numerical approximation of these two special points in the spectrum of the plasma with homogeneous density, we wondered how continua and singular modes would be approximated by the finite element method. A reason why we are looking at these singular modes is the fact that localized regular unstable Suydam-modes, as they appear in a diffuse pinch with current flow, behave quite similarly. Naturally, the maximum number of modes associated with a "continuum" cannot exceed the number of linearly independent vectors with the characteristics of the wave-class in question. This upper bound is approximately given by the number of mesh-points used. In our model, we find $n - 1$ Alfven-modes and $n - n_d - 1$ slow modes, where n_d denotes the number of slow modes associated with discrete eigenvalues. First we show in Fig. 3 how the "singularity" of an Alfven-mode grows, when the number n of intervals is increased. The density parameter ϵ, Eq. (24), is chosen to be 0.1. The modes are normalized numerically by

$$\int_0^R |\xi|^2 r\, dr = 1. \tag{29}$$

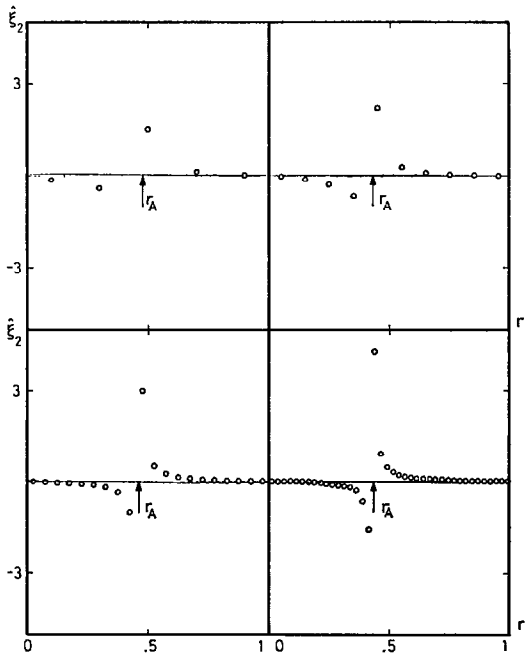

FIG. 3. "Singular" Alfven eigenmodes in the inhomogeneous currentless plasma cylinder with 5, 10, 20, and 40 intervals. Only the dominant component $\hat{\xi}_2$ is given. r_A denotes the analytically determined position of the singularity.

The components $\hat{\xi}_1 = \xi_r$ and $\hat{\xi}_3 = i\xi_z$ being much smaller than the component $\hat{\xi}_2 = (\xi_r + \text{im}\ \xi_\theta)/r$, Fig. 3 shows only the component $\hat{\xi}_2$. The $1/(r - r_A)$ behavior of the mode can clearly be seen. Its maximum amplitude increases ($\propto n^{1/2}$) and its half-width decreases ($\propto 1/n$) with increasing n since no norm for the analytic solution exists:

$$\int_0^R |\ \xi_\theta\ |^2\ r\ dr \propto \int_0^R \frac{1}{(r - r_A)^2}\ r\ dr = \infty. \tag{30}$$

The singular point r_A is defined by the condition $b_A(r_A) = 0$ using the numerical solution to ω and Eq. (26) for b_A. The point r_A lies systematically near the grid point to its right. This phenomenon seems to be inherent in our numerical method as can be seen from Fig. 4. Here all Alfven-modes possible in an equidistant mesh with n intervals are shown. Each mode is characterized by its frequency scaled with $\omega_0^2 = k^2 B_z^2/\rho_0$ and the place r, where the mode is "singular." Numerically the singular point cannot exactly be determined. It lies somewhere between the two grid points, which exhibit the most "singular" behavior. The error-bars in Fig. 4

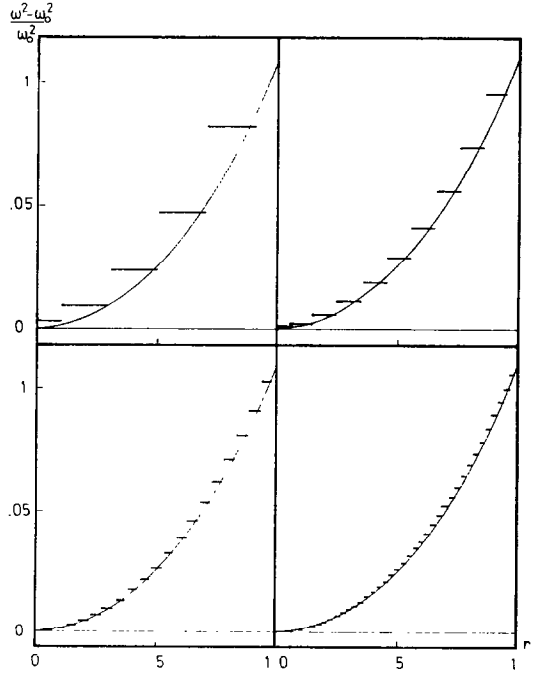

FIG. 4. Numerically detected "continuous" spectrum of the Alfven branch for a density profile with $\epsilon = 0.1$. The numbers of intervals used are 5, 10, 20, and 40, respectively.

make this uncertainty visible. The solid line represents the analytic solution to $b_A(r_A) = 0$.

From Figs. 3 and 4, we conclude that a numerical spectrum may be regarded as continuous in a certain frequency band, if

1° the associated normalized modes have "singularities";

2° the number of modes in a fixed frequency interval increases with increasing number of mesh points;

3° the polygon defined by the mesh points nearest to the "singularities" and the associated frequencies ω^2 of the modes converges to a smooth curve.

As a further demonstration (Fig. 5), we calculate the spectrum of the slow waves. With increasing inhomogeneity, i.e., increasing ϵ, the accumulation point opens to a continuum which eventually covers the discrete eigenvalues. The solid line represents the analytic upper limit, Eq. (28), of the continuum.

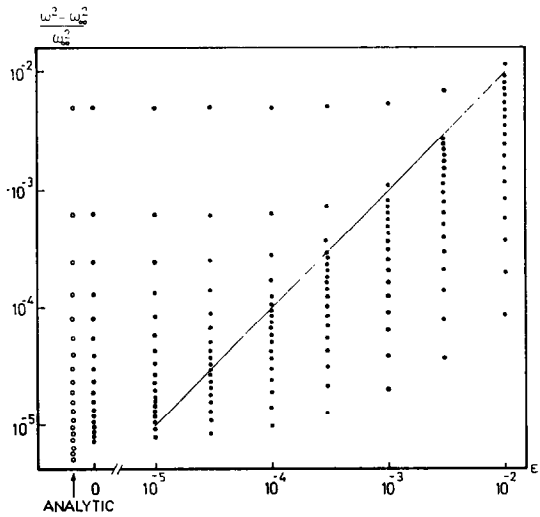

FIG. 5. The spectrum of the slow waves in an inhomogeneous currentless plasma cylinder with varying density profile ϵ. The wavenumbers are $m = 1$ and $k = -0.5$. The solid line represents the analytic limit between the discrete spectrum (upper part) and the continuous spectrum (lower part). At the left-hand side the analytic and numerical spectra are given for $\epsilon = 0$.

A simple Screw-Pinch Model

Finally, we apply our method to an incompressible plasma ($\gamma = \infty$) of constant density ρ lying in a constant longitudinal field B_z and carrying a longitudinal, constant current. The pressure p satisfies the pressure balance, Eq. (2). The sta-

bility theory of such a plasma has been given by Shafranov [25] for $m \geqslant 1$. Takeda *et al.* [2] have tested their finite element method with this model and have found that there might be an error inherent in the numerical formulation. Yet, taking a large number of mesh-points, they were successful in calculating the growth rates of the most unstable modes. We shall show that the discrete space V, Eqs. (19) and (20), should be chosen rather than the space chosen by Takeda *et al.* [2], if good accuracy is desired. Further we shall show that the unstable modes are well approximated within a low-dimensional space V, whereas it is almost impossible to approximate them within the space chosen by Takeda *et al.* [2].

First we quote Shafranov's result for the component ξ_r of an unstable mode

$$\xi_r = \text{const} \left\{ \frac{m}{r} (\mu + 1) J_m[kr(\mu^2 - 1)^{1/2}] - k(\mu^2 - 1)^{1/2} J_{m-1}[kr(\mu^2 - 1)^{1/2}] \right\}. \tag{31}$$

Here $\mu = 2k^2\tau/q(k^2\tau^2 - \omega^2\rho/B_z^2)$, $\tau = 1 - m/q$, and $q = kRB_z/B_\theta(R)$. The boundary condition, Eq. (4), is satisfied for values μ_0, which determine the growth rates of the modes

$$-\omega^2 = (B_z^2k^2/\rho)[(2\tau/\mu_0 q) - \tau^2]. \tag{32}$$

Figure 6 now shows the results for the growth rates ($m = 2, k = -0.2$) obtained by Takeda's and our methods. In both cases, we used an equidistant mesh of 20 intervals. With all linear and continuous basis functions a single unstable mode can be found, whereas in space V there are more than ten. The growth rates of the

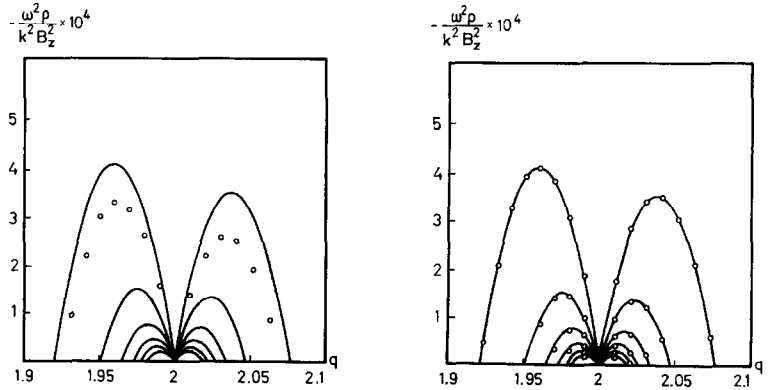

FIG. 6. Growth rates versus q of an incompressible screw-pinch carrying a homogeneous current. The solid lines represent the six most unstable mode pairs as obtained analytically from (24). The corresponding numerical results are indicated by points. At the left-hand side Takeda's method was used.

six most unstable modes (strictly speaking, modepairs) are drawn. They correspond to the following six pairs of μ_0-values: -25.19, 26.19; -41.60, 42.59; -73.49, 74.48; -89.31, 90.30; -105.09, 106.09; -120.86, 121.85. The solid lines represent the analytic solution, Eq. (32). In Fig. 7, then, the analytic and the numerical solutions to the mode form are compared. Once more, our elements and 20 intervals have been used. Figures 6 and 7 demonstrate the good accuracy obtained with the finite element method satisfying, Eq. (18). From Fig. 6 one concludes that the error inherent in the numerical formulation of Takeda *et al.* [2] is caused by the violation of Eq. (18).

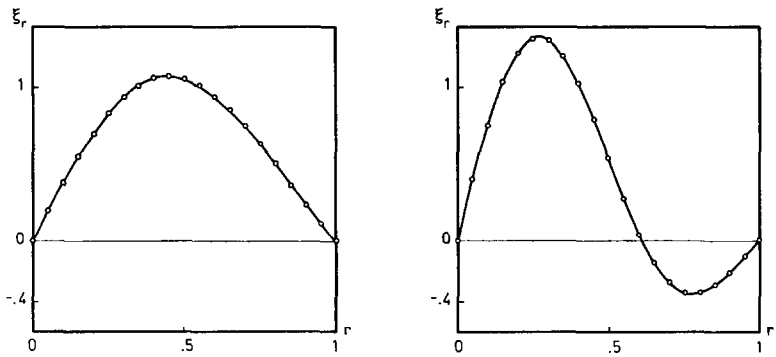

FIG. 7. Analytic (solid line) and numerical (points) solutions of the radial component ξ_r and the two dominant unstable modes at $q = 1.98$.

V. CONCLUSION

We have proposed a new class of very simple basis functions for the finite element approximation of the one-dimensional normal mode MHD-equations. It has been shown that within this function class certain important features of the fixed boundary MHD-problem are exactly or at least intelligibly described by the discrete system. The proposed basis functions are appropriate for extremely local instabilities [26] in complicated equilibrium conditions. They allow the calculation of singular eigenmodes having a continuous spectrum (Section IV) and they even describe correctly the eigenvalues and eigenfunctions of the slow waves (Section IV), i.e., a class of solutions to Eq. (10) with discrete eigenvalues in an extremely narrow frequency band, which are descending toward an accumulation point [4]. Finally, we showed that the instabilities of a screw-pinch with fixed boundary can be calculated with high accuracy even using few mesh-points. The method can equally well be applied to free boundary problems [27].

Originally, the choice of the new basis functions was motivated by our desire to

describe the instabilities of a screw-pinch more accurately. Afterward, we found them to be much more universal. So we believe that they could be useful in other branches of physics and engineering as well. We do not intend to give criteria for their applicability, but we would like to give the following hint: If the variational form of your finite element problem at hand admits a discontinuous basis, try it.

ACKNOWLEDGMENTS

We are indebted to Drs. R. A. Dory and F. Hofmann and to our two referees, who have carefully read and criticized the manuscript. We would also like to thank Professor J. Descloux and Dr. F. Troyon for their helpful comments and discussions. This work was supported by the Swiss National Science Foundation.

REFERENCES

1. M. OHTA, Y. SHIMOMURA, AND T. TAKEDA, *Nucl. Fusion* **12** (1972), 271.
2. T. TAKEDA, Y. SHIMOMURA, M. OHTA, AND M. YOSHIKAWA, *Phys. Fluids* **15** (1972), 2193.
3. T. J. M. BOYD, G. A. GARDNER, AND L. R. T. GARDNER, *Nucl. Fusion* **13** (1973), 764.
4. K. APPERT, D. BERGER, R. GRUBER, F. TROYON, AND J. RAPPAZ, *ZAMP* **25** (1974), 229.
5. C. UBEROI, *Indian J. Pure Appl. Phys.* **2** (1964), 133.
6. D. C. PRIDMORE-BROWN, *Phys. Fluids* **9** (1966), 1290.
7. D. A. MCPHERSON AND D. C. PRIDMORE-BROWN, *Phys. Fluids* **9** (1966), 2033.
8. T. TATARONIS AND W. GROSSMANN, Paper B-5, Proceedings of the Second Topical Conference on Pulsed High-Beta Plasma, IPP-Report 1/127, July, 1972.
9. W. GROSSMANN AND J. TATARONIS, Paper B-6, Proceedings of the Second Topical Conference on Pulsed High-Beta Plasma, IPP-Report 1/127, July, 1972.
10. J. TATARONIS AND W. GROSSMANN, *Z. Physik* **261** (1973), 203.
11. W. GROSSMANN AND J. TATARONIS, *Z. Physik* **261** (1973), 217.
12. H. GRAD, *Proc. Natl. Acad. Sci. U. S.* **70** (1973), 3277.
13. K. APPERT, R. GRUBER, AND J. VACLAVIK, *Phys. Fluids* **17** (1974), 1471.
14. R. L. DEWAR, R. C. GRIMM, J. L. JOHNSON, E. A. FRIEMAN, J. M. GREENE, AND P. H. RUTHERFORD, MATT-1017, Princeton University, 1973.
15. G. SCHMIDT, "Physics of High Temperature Plasmas," Academic Press, New York, 1966.
16. W. A. NEWCOMB, *Ann. Phys. (N.Y.)* **10** (1960), 232.
17. G. STRANG AND G. J. FIX, "An Analysis of the Finite Element Method," Prentice–Hall, Englewood Cliffs, N.J., 1973.
18. J. M. GREENE AND J. L. JOHNSON, Hydromagnetic Equilibrium and Stability, in "Advances in Theoretical Physics" (K. A. Brueckner, Ed.), Vol. 1, p. 195, Academic Press, New York/London, 1965.
19. J. P. GOEDBLOED AND H. J. L. HAGEBEUK, *Phys. Fluids* **15** (1972), 1090.
20. I. B. BERNSTEIN, E. A. FRIEMAN, M. D. KRUSKAL, AND R. M. KULSRUD, *Proc. Roy. Soc. (London), Ser. A* **244** (1958), 39.
21. V. D. SHAFRANOV, *Sov. Phys. Tech. Phys.* **15** (1970), 175.
22. K. APPERT, D. BERGER, R. GRUBER, J. RAPPAZ, AND F. TROYON, *ZAMP* **25** (1974), 116.

23. K. APPERT, D. BERGER, AND R. GRUBER, LRP 76/73, École Polytechnique Fédérale de Lausanne, Centre de Recherches en Physique des Plasmas.
24. E. M. BARSTON, *Ann. Phys. (N.Y.)* **29** (1964), 282.
25. V. D. SHAFRANOV, in "Plasma Physics and the Problem of Controlled Thermonuclear Reactions," Vol. IV, p. 71, Pergamon Press, London, 1960.
26. K. APPERT, D. BERGER, AND R. GRUBER, *Phys. Letters* **46A** (1974), 339.
27. K. APPERT, D. BERGER, R. GRUBER, K. V. ROBERTS, AND F. TROYON, LRP 87/74, École Polytechnique Fédérale de Lausanne, Centre de Recherches en Physique des Plasmas.